Eur. Phys. J. A **18**, 185–187 (2003)
DOI 10.1140/epja/i2002-10297-y

THE EUROPEAN PHYSICAL JOURNAL A

S = −1 meson-baryon scattering in coupled-channel unitarized Chiral Perturbation Theory*

C. García-Recio[1], J. Nieves[1], E. Ruiz Arriola[1,a], and M. Vicente Vacas[2]

[1] Departamento de Física Moderna, Universidad de Granada, E-18071 Granada, Spain
[2] Departamento de Física Teórica and IFIC, Centro Mixto Universidad de Valencia-CSIC, Ap. Correos 22085, E-46071 Valencia, Spain

Received: 30 September 2002 /
Published online: 22 October 2003 – © Società Italiana di Fisica / Springer-Verlag 2003

Abstract. The s-wave meson-baryon scattering amplitude is analyzed for the strangeness $S = -1$ and isospin $I = 0$ sector in a Bethe-Salpeter coupled-channel formalism incorporating Chiral Symmetry. Four two-body channels have been considered: $\bar{K}N$, $\pi\Sigma$, $\eta\Lambda$, $K\Xi$. The needed two-particle irreducible matrix amplitude is taken from lowest-order Chiral Perturbation Theory in a relativistic formalism. Off-shell behaviour is parameterized in terms of low-energy constants, which outnumber those assumed in previous works and provide a better fit to the data. The position of the complex poles in the second Riemann sheet of the scattering amplitude determines masses and widths of the $\Lambda(1405)$ and $\Lambda(1670)$ resonances which compare well with accepted numbers.

PACS. 11.10.St Bound and unstable states; Bethe-Salpeter equations – 11.30.Rd Chiral symmetries – 11.80.Et Partial-wave analysis – 13.75.Lb Meson-meson interactions

1 Introduction

The existence of baryon resonances is a non-perturbative feature of intermediate energy QCD. In addition to the standard relativistic invariance, Chiral Symmetry (CS) and unitarity prove extremely convenient tools to deal with this problem. In this energy range, hadronic degrees of freedom seem to be the relevant ones in terms of which the symmetries may be easily incorporated [1]. Heavy Baryon Chiral Perturbation Theory (HBChPT) [2, 3] incorporates CS at low energies in a systematic way, and has provided a satisfactory description of πN scattering in the region around threshold [4–6] but fails to reproduce the resonance region. The s-wave meson-baryon scattering for the strangeness $S = -1$ and isospin $I = 0$ sector incorporating CS and unitarization has been studied in previous works [7–13]. The need for unitarization in this reaction becomes obvious after the work of ref. [14], where it is shown that HBChPT to one loop fails completely in the $\bar{K}N$ channel already at threshold due to nearby subthreshold $\Lambda(1405)$-resonance.

We report here on results obtained for the s-wave $S = -1$, $I = 0$ meson-baryon reaction in a Bethe-Salpeter Equation (BSE) coupled-channel approach, extending the works of refs. [15–17]. We also improve on a previous approach [8] by reparameterizing off-shell effects as low-energy constants, in the spirit of an Effective Field Theory. We consider four coupled channels: $\pi\Sigma$, $\bar{K}N$, $\eta\Lambda$ and $K\Xi$ and take into account $SU(3)$-breaking symmetry effects but assume isospin symmetry. More details can be found in ref. [18].

2 Theoretical framework

The coupled-channel scattering amplitude for the baryon-meson process in the isospin channel $I = 0$ is given by

$$T_P = \bar{u}_B(P-k', s_B)\, t_P(k,k')\, u_A(P-k, s_A) \qquad (1)$$

Here, $u_A(P-k, s_A)$ and $u_B(P-k', s_B)$ are baryon Dirac spinors normalized as $\bar{u}u = 2M$, P is the conserved total CM four-momentum, $P^2 = s$, and $t_P(k,k')$ is a matrix in the Dirac and coupled-channel spaces. Further details on normalizations and definitions of the amplitudes can be seen in ref. [17]. To evaluate the amplitude t_P we solve the BSE

$$t_P(k,k') = v_P(k,k') + i\int \frac{\mathrm{d}^4 q}{(2\pi)^4} t_P(q,k')\Delta(q)S(P-q)v_P(k,q)\,, \qquad (2)$$

where $t_P(k,k')$ is the scattering amplitude defined in eq. (1), $v_P(k,k')$ the two-particle irreducible Green's function (or *potential*), and $S(P-q)$ and $\Delta(q)$ the baryon and

* Spokesperson: E. Ruiz Arriola.
[a] e-mail: earriola@ugr.es

meson exact propagators, respectively. The above equation turns out to be a matrix one, both in the coupled-channel and Dirac spaces. For any choice of the *potential* $v_P(k,k')$, the resulting scattering amplitude $t_P(k,k')$ fulfills the coupled-channel unitarity condition, discussed in eq. (21) of ref. [17]. The BSE requires some input potential and baryon and meson propagators to be solved. At lowest-order of the BSE-based chiral expansion [15], we approximate the iterated *potential* by the chiral expansion lowest order meson-baryon amplitudes in the desired strangeness and isospin channels, and the intermediate particle propagators by the free ones (which are diagonal in the coupled-channel space). From the meson-baryon chiral Lagrangian [1] (see sect. IIA of ref. [17]), one gets at lowest order for the *potential*:

$$v_P(k,k') = t_P^{(1)}(k,k') = \frac{D}{f^2}(\not{k} + \not{k}') \tag{3}$$

with D the coupled-channel matrix,

$$D = \frac{1}{4} \begin{array}{c} \begin{matrix} \bar{K}N & \pi\Sigma & \eta\Lambda & K\Xi \end{matrix} \\ \begin{pmatrix} -3 & \sqrt{\frac{3}{2}} & -\frac{3}{\sqrt{2}} & 0 \\ \sqrt{\frac{3}{2}} & -4 & 0 & -\sqrt{\frac{3}{2}} \\ -\frac{3}{\sqrt{2}} & 0 & 0 & \frac{3}{\sqrt{2}} \\ 0 & -\sqrt{\frac{3}{2}} & +\frac{3}{\sqrt{2}} & -3 \end{pmatrix} \end{array} \begin{matrix} \bar{K}N \\ \pi\Sigma \\ \eta\Lambda \\ K\Xi \end{matrix} . \tag{4}$$

The s-wave BSE can be solved and renormalized up to a numerical matrix inversion in the coupled-channel space [16].

3 Numerical results

We use the following numerical values for masses and weak decay constants of the pseudoscalar mesons (all in MeV), $m_K = m_{\bar{K}} = 493.68$, $m_\pi = 139.57$, $m_\eta = 547.3$, $M_p = 938.27$, $M_\Sigma = 1189.37$, $M_\Lambda = 1115.68$, $M_\Xi = 1318.0$ and $f_\pi = f_\eta = f_K = 1.15 \times 93.0$, where for the weak meson decay constants we take for all channels an averaged value.

3.1 Fitting procedure

We perform a χ^2-fit, with 12 free parameters, to the following set of experimental data and conditions:

1. $S_{01}(L_{2T2J})$ $\bar{K}N \to \bar{K}N$ and $\bar{K}N \to \pi\Sigma$ scattering amplitudes (real and imaginary parts) [19] in the CM energy range $1480\,\text{MeV} \leq \sqrt{s} \leq 1750\,\text{MeV}$. In this CM energy region, there are a total number of 56 data points (28 real and 28 imaginary parts) for each channel. The normalization used in ref. [19] is different from that used here and their amplitudes, T_{ij}^{Go77}, are related to ours by $T_{ij}^{\text{Go77}} = \text{sig}(i,j)|\boldsymbol{k}_i| \left[f_0^{\frac{1}{2}}(s)\right]_{j\leftarrow i}$, where $\text{sig}(i,j)$ is $+1$ for the elastic channel and -1 for the $\bar{K}N \to \pi\Sigma$ one. On the other hand, and because in ref. [19] errors are not provided, we have taken for those amplitudes errors given by $\delta T_{ij}^{\text{Go77}} = \sqrt{(0.12\ T_{ij}^{\text{Go77}})^2 + 0.05^2}$ in the spirit of those used in ref. [11].
2. $S_{01} - \pi\Sigma$ mass spectrum [20], $1330\,\text{MeV} \leq \sqrt{s} \leq 1440\,\text{MeV}$. In this CM energy region, there are a total of thirteen 10 MeV bins and the experimental data are given in arbitrary units. To compare with data, taking into account the experimental acceptance of 10 MeV, we compute

$$\Delta\sigma/\Delta[M_{\pi\Sigma}(i)] = C \int_{M^-}^{M^+} \left| \left[f_0^{\frac{1}{2}}(s = x^2) \right]_{2\leftarrow 2} \right|^2 \times |\boldsymbol{k}_2(s = x^2)|\ x^2\ \mathrm{d}x\,, \tag{5}$$

where C is an arbitrary global normalization factor[1], $M^\pm = M_{\pi\Sigma}(i) \pm 5\,\text{MeV}$ and i denotes the bin with central CM energy $M_{\pi\Sigma}(i)$. Hence, there are only 12 independent data points. Finally, we take the error of the number of counts, N_i, of the bin i to be $1.61\sqrt{N_i}$ as in ref. [21].
3. The $K^-p \to \eta\Lambda$ total cross-section of ref. [22], $1662\,\text{MeV} \leq \sqrt{s} \leq 1684\,\text{MeV}$. We use the Crystal Ball Collaboration precise new total cross-section measurements (a total of 17 data points compiled in table I of ref. [22]) for the near-threshold reaction $K^-p \to \eta\Lambda$, which is dominated by the $\Lambda(1670)$-resonance. We assume, as in ref. [22], that the p- and higher wave contributions do not contribute to the total cross-section.

Finally, we define the χ^2, which is minimized, as

$$\chi^2/N_{\text{tot}} = \frac{1}{N}\sum_{\alpha=1}^{N} \frac{1}{n_\alpha} \sum_{j=1}^{n_\alpha} \left(\frac{x_j^{(\alpha)\,\text{th}} - x_j^{(\alpha)}}{\sigma_j^{(\alpha)}} \right)^2 , \tag{6}$$

where $N = 4$ stands for the four sets of data used and discussed above. Though we have considered four coupled channels, three-body channels, for instance the $\pi\pi\Sigma$ one, are not explicitly considered, as has been also assumed previously in refs. [12] and [22]. The fit is shown in fig. 1.

3.2 Poles and couplings

Resonances are defined as poles in the second Riemann sheet of the s-complex plane. Around them, the scattering matrix behaves as

$$[t(s)]_{ij} \to \frac{2M_R g_i g_j}{s - M_R^2 + \mathrm{i}M_R\Gamma_R}\,. \tag{7}$$

We find three poles in the second Riemann sheet whose positions are given in table 1. Errors have been transported

[1] We fix it by setting the area of our theoretical spectrum, $\sum_i \frac{\Delta\sigma}{\Delta[M_{\pi\Sigma}(i)]}$, to the total number of experimental counts $\sum_i N_i$.

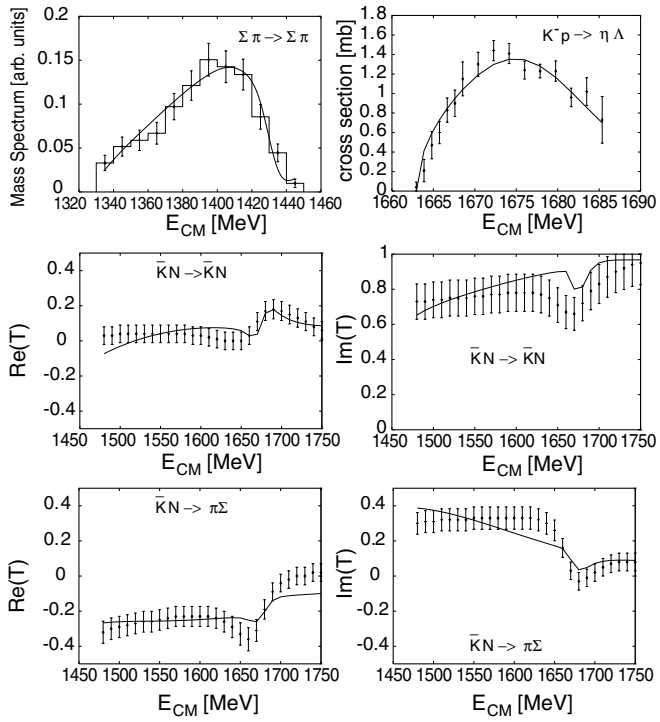

Fig. 1. Best-fit results for the Bethe-Salpeter Equation in the $S = -1$, $I = 0$ channel (solid lines). Upper panel: Experimental data for $\pi\Sigma \to \pi\Sigma$ and $K^- p \to \eta\Lambda$ are from refs. [20] and [22], respectively. Middle panel: The real (left panel) and imaginary (right panel) parts of the s-wave T-matrix, with normalization specified in the main text, for elastic $\bar{K}N \to \bar{K}N$ process in the $I = 0$ isospin channel as functions of the CM energy. Experimental data are taken from the analysis of ref. [19] with the errors stated in the main text. Lower panel: Same as middle panel for the inelastic channel $\bar{K}N \to \pi\Sigma$.

Table 1. Resonance masses and widths (in MeV).

	First	Second	Third
M_R	1368 ± 12	1443 ± 3	1677.5 ± 0.8
Γ_R	250 ± 20	50 ± 7	29.2 ± 1.4

from those in the best-fit parameters [18], taking into account the existing statistical correlations through a Monte Carlo simulation. As can be seen from fig. 2 besides the three poles appearing in the second Riemann sheet, unphysical poles show up in the physical sheet out of the real axis, but they do not influence the scattering. Our resonances are not of the Breit-Wigner form. For the $\Lambda(1670)$-resonance, branching ratios, as defined in ref. [18], are

$$B_{\bar{K}N} = 0.24, \qquad B_{\pi\Sigma} = 0.08, \qquad B_{\eta\Lambda} = 0.68\,. \quad (8)$$

These values reasonably agree with the values quoted in the PDG ($B_{\bar{K}N} = 0.20 \pm 0.05,\ B_{\pi\Sigma} = 0.40 \pm 0.20,\ B_{\eta\Lambda} = 0.25 \pm 0.10$) and in ref. [23] ($B_{\bar{K}N} = 0.37 \pm 0.07,\ B_{\pi\Sigma} = 0.16 \pm 0.06,\ B_{\eta\Lambda} = 0.39 \pm 0.08,\ B_{\pi\Sigma(1385)} = 0.08 \pm 0.06$).

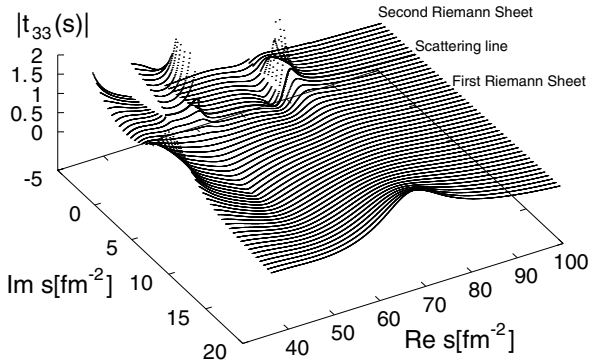

Fig. 2. Modulus of the $\eta\Lambda \to \eta\Lambda$ element of the scattering amplitude $t(s)$ (fm), analytically extended to the first and fourth quadrants of the s-complex plane. The solid line is the scattering line, $s + \mathrm{i}\ 0^+$, from the first threshold, $(m_\pi + M_\Sigma)^2$, on. The first (second) Riemann sheet is depicted in the first (fourth) quadrant of the s-complex plane.

This work has been supported by the DGES grants no. BFM200-1326 and PB98-1367 and the Junta de Andalucía.

References

1. A. Pich, Rep. Prog. Phys. **58**, 563 (1995).
2. E. Jenkins, A.V. Manohar, Phys. Lett. B **255**, 558 (1991).
3. V. Bernard, N. Kaiser, J. Kambor, Ulf G. Meissner, Nucl. Phys. B **388**, 315 (1992).
4. M. Mojzis, Eur. Phys. J. C **2**, 181 (1998).
5. N. Fettes, Ulf-G. Meissner, S. Steininger, Nucl. Phys. A **640**, 199 (1988).
6. N. Fettes, Ulf G. Meißner, Nucl. Phys. A **676**, 311 (2000).
7. N. Kaiser, P.B. Siegel, W. Weise, Nucl. Phys. A **594**, 325 (1995).
8. E. Oset, A. Ramos, Nucl. Phys. A **635**, 99 (1998).
9. B. Krippa, Phys. Rev. C **58**, 1333 (1998).
10. J.A. Oller, Ulf G. Meißner, Phys. Lett. **500**, 263 (2001).
11. M.Th. Keil, G. Penner, U. Mosel, Phys. Rev. C **63**, 045202 (2001).
12. E. Oset, A. Ramos, C. Bennhold, Phys. Lett. B **522**, 260 (2002).
13. M.F.M. Lutz, E.E. Kolomeitsev, Nucl. Phys. A **700**, 193 (2002).
14. N. Kaiser, Phys. Rev. **C 64** , 045204 (2001).
15. J. Nieves, E. Ruiz Arriola, Phys. Lett. B **455**, 30 (1999); Nucl. Phys. A **679**, 57 (2000).
16. J. Nieves, E. Ruiz Arriola, Phys. Rev. D **63**, 076001 (2001).
17. J. Nieves, E. Ruiz Arriola, Phys. Rev. D **64**, 481 (2001).
18. C. García Recio, J. Nieves, E. Ruiz Arriola, M. J. Vicente-Vacas, work in preparation.
19. G.P. Gopal *et al.*, Nucl. Phys. B **119**, 362 (1977).
20. R.J. Hemingway, Nucl. Phys. B **253**, 742 (1984).
21. R.H. Dalitz, A. Deloff, J. Phys. G **17**, 289 (1991).
22. A. Starostin *et al.*, Phys. Rev. C **64**, 055205 (2001).
23. D.M. Manley *et al.*, Phys. Rev. Lett. **88**, 012002-1 (2002).